

Nuclear symmetry energy in a modified quark meson coupling model

R.N. Mishra,¹ H.S. Sahoo,¹ P.K. Panda,² N. Barik,² and T. Frederico³

¹*Department of Physics, Ravenshaw University, Cuttack-753 003, India*

²*Department of Physics, Utkal University, Bhubaneswar-751 004, India*

³*Departamento de Física, Instituto Tecnológico de Aeronáutica, 12228-900 São José dos Campos, SP, Brazil*

We study nuclear symmetry energy and the thermodynamic instabilities of asymmetric nuclear matter in a self-consistent manner by using a modified quark-meson coupling model where the confining interaction for quarks inside a nucleon is represented by a phenomenologically averaged potential in an equally mixed scalar-vector harmonic form. The nucleon-nucleon interaction in nuclear matter is then realized by introducing additional quark couplings to σ , ω , and ρ mesons through mean-field approximations. We find an analytic expression for the symmetry energy \mathcal{E}_{sym} as a function of its slope L . Our result establishes a linear correlation between L and \mathcal{E}_{sym} . We also analyze the constraint on neutron star radii in (pn) matter with β equilibrium.

PACS numbers: 26.60.+c, 21.30.-x, 21.65.Qr, 95.30.Tg

I. INTRODUCTION

One of the major focuses in the study of nuclear matter has recently been to understand the equation of state (EOS) of asymmetric nuclear matter and the density dependence of the nuclear symmetry energy. The nuclear symmetry energy is a fundamental quantity which determines several important properties of very small entities such as the atomic nuclei as well as very large objects such as neutron stars [1]. In fact, the behavior of nuclear symmetry energy is most uncertain among all properties of dense nuclear matter. Furthermore, the symmetry energy is important for modeling nuclear matter by probing the isospin part of nuclear interactions. Recent [2] experimental studies of isospin-sensitive observables in intermediate-energy nuclear reactions involving radioactive beams have been quite useful in providing some constraints on the density dependence of nuclear symmetry energy at subsaturation densities. The effects of symmetry energy and its slope on neutron star properties is an important area of study. Another area of relevance in the study of asymmetric nuclear matter is the instabilities associated with possible liquid-gas phase transitions at subsaturation densities. Such liquid-gas phase transition plays an important role in the description of the crust of compact star matter at densities between 0.03 fm^{-3} and saturation density (0.15 fm^{-3}). Here, we would like to address these two relevant aspects in the study of asymmetric nuclear matter in a phenomenological model that we have used in our earlier work for symmetric nuclear matter.

There has been a proliferation of phenomenological models to describe infinite nuclear matter and also properties of finite nuclei. These are in fact essential steps in the development of this area of study for which realistic first-principles theoretical descriptions as well as adequate experimental or observational data are not available. Variations in different phenomenological approaches stretching from the nonrelativistic to the rel-

ativistic are tried incorporating some further aspects of theoretical requirements in the model. All these models are usually set in terms of parameters that are fit to reproduce the properties of either finite nuclei [3] or bulk nuclear matter. As a result, most of the models behave more or less similarly as far as the equation of state is concerned around the saturation density and at zero temperature. However, when these models are used to describe nuclear matter at subsaturation densities to explain the liquid-gas phase transition or at high densities to explain neutron star matter, they yield very different results. Therefore, it has been seen as essential to incorporate some constraints related to symmetry energy and its derivatives by using up-to-date theoretical and experimental information. Most of the relativistic-mean-field (RMF) models are attempts in these directions. However, in these models nucleons are treated as structureless point objects. Therefore, as a next step in the requirement of incorporating the quark structure of the nucleon with meson couplings at the basic level; quark-meson-coupling (QMC) models have been proposed [4] and properties of nuclear matter have been studied in great detail in a series of works [5–8]. In these models nucleons are described as a system of nonoverlapping MIT bags which interact through effective scalar and vector meson exchanges at the quark level. However, it has been argued that the hadronic structure described by the MIT-bag model suffers from some theoretical inadequacy due to the sharp bag boundary in breaking chiral symmetry, which is a good symmetry of strong interactions within the partially conserved axial current (PCAC) limit. Therefore, more sophisticated versions such as the Cloudy Bag Model (CBM) have been proposed for the study of hadronic structure. So, to further include this aspect of the physics requirement, it would be more appropriate to develop a quark-meson coupling model where nucleon structure is described by models like the CBM instead of by MIT bags. As an alternative approach [9–11] to the CBM, the relativistic independent

quark model with a phenomenologically averaged confining potential in equally mixed scalar-vector harmonic form in the Dirac frame work has been used extensively with remarkable consistency in the baryonic as well as the mesonic sector [12]. This model has provided a very suitable alternative to the otherwise successful cloudy bag model in describing hadronic structure with its static properties and various decay properties.

We therefore proposed in our earlier work [13] a modified quark-meson coupling model (MQMC), which is based on a suitable confining relativistic independent quark potential rather than a bag to address the nucleon structure in vacuum as an alternative approach to QMC for the study of symmetric nuclear matter. This attempt was not so much as to plead superiority of MQMC over QMC at this level. It has only incorporated an essential aspect of the physics requirement missing in MIT-bag model to stand as an alternative to the more appropriate CBM. Further investigations are necessary to check its consistency and its predictability for any new physical features. In the MQMC model, we have studied the bulk nuclear properties such as the compressibility, the structure of EOS, and also discussed some implications of chiral symmetry in nuclear matter along with the nucleon and nuclear Σ term and the sensitivity of nuclear matter binding energy with variations in the light quark mass. The results obtained in such a picture for symmetric nuclear matter were quite encouraging. In the present attempt, we study the bulk properties of asymmetric nuclear matter and also the low-density instabilities of the system in such a model. To treat the asymmetric nuclear matter, we incorporate in our model the contribution of the isovector vector meson ρ in addition to those of the isoscalar scalar meson (σ) and isoscalar vector meson (ω) considered earlier for symmetric nuclear matter [13]. Such studies are also useful to discuss the systems such as neutron stars with $N \neq Z$.

A correlation between the symmetry energy \mathcal{E}_{sym} and its slope L has been verified recently by Ducoin *et al.* [14] for a set of effective relativistic and nonrelativistic nuclear models. Such a study was based on numerical results for \mathcal{E}_{sym} and L obtained from different parametrizations. Theoretically \mathcal{E}_{sym} and L are constrained [15, 16]. In a recent paper, Santos *et al.* [17] have established an analytic relationship between these quantities. In this context QMC-based models have not been studied. We have made an attempt to set up a relationship between these two quantities analytically.

The paper is organized as follows: In Sec. II, a brief outline of the model describing the nucleon structure in vacuum is discussed. The nucleon mass is then realized by appropriately taking into account the center-of-mass correction, pionic correction, and gluonic correction. The EOS is then developed. In Sec. III, we discuss the nuclear symmetry energy, its slope and incompressibility, and observe its density dependence. The thermodynamic instabilities of the system are analyzed in Sec. IV. We

establish the analytic relationship between \mathcal{E}_{sym} and L and discuss the results in Sec. V.

II. MODIFIED QUARK MESON COUPLING MODEL

Recently, the modified quark-meson coupling model was adopted for symmetric nuclear matter where the NN interaction was realized in a mean-field approach through the exchange of effective (σ, ω) mesonic fields coupling to the quarks inside the nucleon [13]. We now extend this model to asymmetric nuclear matter and include the contribution of the isovector vector meson, ρ , in addition to σ and ω mesons. In view of this, we briefly present the outlines of our approach [13] in the present context.

We first consider nucleons as a composite of constituent quarks confined in a phenomenological flavor-independent confining potential, $U(r)$ in an equally mixed scalar and vector harmonic form inside the nucleon [13], where

$$U(r) = \frac{1}{2}(1 + \gamma^0)V(r),$$

with

$$V(r) = (ar^2 + V_0), \quad a > 0. \quad (1)$$

Here (a, V_0) are the potential parameters. The confining interaction here provides the zeroth-order quark dynamics of the hadron. In the medium, the quark field $\psi_q(\mathbf{r})$ satisfies the Dirac equation

$$[\gamma^0 (\epsilon_q - V_\omega - \frac{1}{2}\tau_{3q}V_\rho) - \vec{\gamma} \cdot \vec{p} - (m_q - V_\sigma) - U(r)]\psi_q(\vec{r}) = 0 \quad (2)$$

where $V_\sigma = g_\sigma^q \sigma_0$, $V_\omega = g_\omega^q \omega_0$ and $V_\rho = g_\rho^q b_{03}$; where σ_0 , ω_0 , and b_{03} are the classical meson fields, and g_σ^q , g_ω^q , and g_ρ^q are the quark couplings to the σ , ω , and ρ mesons, respectively. m_q is the quark mass and τ_{3q} is the third component of the Pauli matrices. In the present paper, we consider nonstrange $q = u$ and d quarks only. We can now define

$$\epsilon'_q = (\epsilon_q^* - V_0/2) \quad \text{and} \quad m'_q = (m_q^* + V_0/2), \quad (3)$$

where the effective quark energy, $\epsilon_q^* = \epsilon_q - V_\omega - \frac{1}{2}\tau_{3q}V_\rho$ and effective quark mass, $m_q^* = m_q - V_\sigma$. We now introduce λ_q and r_{0q} as

$$(\epsilon'_q + m'_q) = \lambda_q \quad \text{and} \quad r_{0q} = (a\lambda_q)^{-\frac{1}{4}}. \quad (4)$$

The ground-state quark energy can be obtained from the eigenvalue condition

$$(\epsilon'_q - m'_q)\sqrt{\frac{\lambda_q}{a}} = 3. \quad (5)$$

The solution of equation (5) for the quark energy ϵ_q^* immediately leads to the mass of the nucleon in the medium in zeroth order as

$$E_N^{*0} = \sum_q \epsilon_q^* \quad (6)$$

We next consider the spurious center-of-mass correction $\epsilon_{c.m.}$, the pionic correction δM_N^π for restoration of chiral symmetry, and the short-distance one-gluon exchange contribution $(\Delta E_N)_g$ to the zeroth-order nucleon mass in the medium. The center-of-mass correction $\epsilon_{c.m.}$ and the pionic corrections δM_N^π in the present model are found, respectively, as [13]

$$\epsilon_{c.m.} = \frac{(77\epsilon'_u + 31m'_u)}{3(3\epsilon'_u + m'_u)^2 r_{0u}^2} \quad (7)$$

and

$$\delta M_N^\pi = -\frac{171}{25} I_\pi f_{NN\pi}^2. \quad (8)$$

Here,

$$I_\pi = \frac{1}{\pi m_\pi^2} \int_0^\infty dk \frac{k^4 u^2(k)}{w_k^2}, \quad (9)$$

with the axial vector nucleon form factor given as

$$u(k) = \left[1 - \frac{3}{2} \frac{k^2}{\lambda_q(5\epsilon'_q + 7m'_q)} \right] e^{-k^2 r_0^2/4}. \quad (10)$$

The pseudovector nucleon pion coupling constant $f_{NN\pi}$ can be obtained from the familiar Goldberg Triemann relation by using the axial-vector coupling-constant value g_A in the model, as discussed in Ref. [13].

The color-electric and color-magnetic contributions to the gluonic correction which arises due to one-gluon exchange at short distances are given as:

$$(\Delta E_N)_g^E = \alpha_c (b_{uu} I_{uu}^E + b_{us} I_{us}^E + b_{ss} I_{ss}^E), \quad (11)$$

and due to color-magnetic contributions, as

$$(\Delta E_N)_g^M = \alpha_c (a_{uu} I_{uu}^M + a_{us} I_{us}^M + a_{ss} I_{ss}^M), \quad (12)$$

where a_{ij} and b_{ij} are the numerical coefficients depending on each baryon. The color-electric contributions to the correction of baryon masses due to one gluon exchange are calculated in a field-theoretic manner [13]. It can be found that the numerical coefficient for color-electric contributions such as b_{uu} , b_{us} , and b_{ss} comes out to be zero. From calculations we have $a_{uu} = -3$ and $a_{us} = a_{ss} = b_{uu} = b_{us} = b_{ss} = 0$ for the nucleons. The quantities I_{ij}^E and I_{ij}^M are given in the following equation

$$I_{ij}^E = \frac{16}{3\sqrt{\pi}} \frac{1}{R_{ij}} \left[1 - \frac{\alpha_i + \alpha_j}{R_{ij}^2} + \frac{3\alpha_i \alpha_j}{R_{ij}^4} \right],$$

$$I_{ij}^M = \frac{256}{9\sqrt{\pi}} \frac{1}{R_{ij}^3} \frac{1}{(3\epsilon'_i + m'_i)} \frac{1}{(3\epsilon'_j + m'_j)}, \quad (13)$$

where

$$R_{ij}^2 = 3 \left[\frac{1}{(\epsilon'_i{}^2 - m'_i{}^2)} + \frac{1}{(\epsilon'_j{}^2 - m'_j{}^2)} \right]$$

$$\alpha_i = \frac{1}{(\epsilon'_i + m'_i)(3\epsilon'_i + m'_i)}. \quad (14)$$

In the calculation we have taken $\alpha_c = 0.58$ as the strong-coupling constant in QCD at the nucleon scale [10]. The color-electric contribution is zero here, and the gluonic corrections to the mass of the nucleon are due to color-magnetic contributions only.

Finally, treating all these corrections independently, the mass of the nucleon in the medium becomes

$$M_N^* = E_N^{*0} - \epsilon_{c.m.} + \delta M_N^\pi + (\Delta E_N)_g^E + (\Delta E_N)_g^M. \quad (15)$$

The total energy density and pressure at a particular baryon density for the nuclear matter becomes

$$\mathcal{E} = \frac{1}{2} m_\sigma^2 \sigma_0^2 + \frac{1}{2} m_\omega^2 \omega_0^2 + \frac{1}{2} m_\rho^2 b_{03}^2$$

$$+ \frac{\gamma}{(2\pi)^3} \sum_{N=p,n} \int^{k_{f,N}} d^3k \sqrt{k^2 + M_N^{*2}}, \quad (16)$$

$$P = -\frac{1}{2} m_\sigma^2 \sigma_0^2 + \frac{1}{2} m_\omega^2 \omega_0^2 + \frac{1}{2} m_\rho^2 b_{03}^2$$

$$+ \frac{\gamma}{3(2\pi)^3} \sum_{N=p,n} \int^{k_{f,N}} \frac{k^2 d^3k}{\sqrt{k^2 + M_N^{*2}}}, \quad (17)$$

where $\gamma = 2$ is the spin degeneracy factor for nuclear matter. The nucleon density becomes

$$\rho_N = \frac{\gamma}{(2\pi)^3} \int_0^{k_{f,N}} d^3k = \frac{\gamma k_{f,N}^3}{6\pi^2} \quad \text{where } N = p, n. \quad (18)$$

Therefore, the total baryon density becomes $\rho_B = \rho_p + \rho_n$ and the (third component of) isospin density $\rho_3 = \rho_p - \rho_n$. The proton fraction, y_p is defined as

$$y_p = \frac{\rho_p}{\rho_B} \quad (19)$$

where ρ_p and ρ_n are the proton and neutron densities.

The vector mean-fields ω_0 and b_{03} are determined through

$$\omega_0 = \frac{g_\omega}{m_\omega^2} \rho_B \quad b_{03} = \frac{g_\rho}{2m_\rho^2} \rho_3, \quad (20)$$

where $g_\omega = 3g_\omega^q$ and $g_\rho = g_\rho^q$. Finally, the scalar mean-field σ_0 is fixed by

$$\frac{\partial \mathcal{E}}{\partial \sigma_0} = 0. \quad (21)$$

The iso-scalar scalar and iso-scalar vector couplings g_σ^q and g_ω are fit to the saturation density and binding energy for nuclear matter. The isovector vector coupling g_ρ is set by fixing the symmetry energy. For a given baryon density, ω_0 , b_{03} , and σ_0 are calculated from Eqs. (20) and (21), respectively.

III. THE SYMMETRY ENERGY

We may define the neutron-excess parameter $t = \frac{\rho_n - \rho_p}{\rho_n + \rho_p} = (1 - 2y_p)$ so that the nuclear symmetry energy \mathcal{E}_{sym} can be obtained as the difference between the total energy per baryon $\mathcal{E}/\rho_B = E(\rho_B, t)$ of pure neutron matter and that of isospin-symmetric matter at baryon density ρ_B . Here we consider the nuclear matter consisting of protons and neutrons only with y_p as the proton fraction. An expansion of the total energy per baryon, $E(\rho_B, t)$, with respect to the neutron-excess parameter, becomes [18]

$$E(\rho_B, t) = E(\rho_B, 0) + tE_1(\rho_B) + \frac{t^2}{2!}E_2(\rho_B) + \frac{t^3}{3!}E_3(\rho_B) + \dots, \quad (22)$$

where E_1, E_2, E_3, \dots , etc. are the first-, second- and third- order derivatives with respect to t in a Taylor's expansion. However, neglecting Coulomb contributions near the isospin symmetry of QCD, demands the total energy of pure neutron matter to be same as that of pure proton matter, for which the odd powers in t are to be forbidden in the above expansion. Again for densities near or below the saturation density ($\rho_B = \rho_0$), truncation of this expansion to quadratic terms in t is considered to be a good approximation. In view of that, the coefficient of the quadratic term in t can be identified as the symmetry energy

$$\mathcal{E}_{sym}(\rho_B) = \frac{1}{2} \left[\frac{\partial^2 E(\rho_B)}{\partial t^2} \right]_{t=0} = \frac{k_{f,N}^2}{6E_{f,N}^*} + \frac{g_\rho^2}{8m_\rho^2} \rho_B, \quad (23)$$

where $E_{f,N}^* = (k_{f,N}^2 + M_N^{*2})^{1/2}$.

This may be considered to be a good approximation even for small proton fraction y_p , which can be valid for finite nuclei. But for nuclear matter at densities in excess of the saturation density ρ_0 , effects of higher order than quadratic in the expansion may be important. Therefore, in order to study the density dependence of $\mathcal{E}_{sym}(\rho_B)$, one may expand this as a function of ρ_B around saturation density ρ_0 in terms of a parameter $x = \frac{(\rho_B - \rho_0)}{3\rho_0}$ to obtain

$$\mathcal{E}_{sym}(\rho_B) = J + xL^0 + \frac{x^2}{2!}K_{sym}^0 + \frac{x^3}{3!}Q_{sym}^0 + \dots, \quad (24)$$

so as to consider the symmetry-energy parameters as fol-

lows:

$$\begin{aligned} J &= \mathcal{E}_{sym}(\rho_0) \\ L^0 &= 3\rho_0 \left. \frac{\partial \mathcal{E}_{sym}(\rho_B)}{\partial \rho_B} \right|_{\rho_B=\rho_0} \quad (\text{Slope of } \mathcal{E}_{sym}) \\ K_{sym}^0 &= 9\rho_0^2 \left. \frac{\partial^2 \mathcal{E}_{sym}(\rho_B)}{\partial \rho_B^2} \right|_{\rho_B=\rho_0} \quad (\text{Curvature of } \mathcal{E}_{sym}) \\ Q_{sym}^0 &= 27\rho_0^3 \left. \frac{\partial^3 \mathcal{E}_{sym}(\rho_B)}{\partial \rho_B^3} \right|_{\rho_B=\rho_0} \quad (\text{Skewness of } \mathcal{E}_{sym}) \end{aligned} \quad (25)$$

Apart from the quantities in Eq. (25), the following quantities calculated from pressure P and energy density \mathcal{E} for the consideration of constraints and correlations studies are

$$\begin{aligned} K_0 &= 9 \left[\frac{dP}{d\rho_B} \right]_{\rho_B=\rho_0, y_p=1/2} \quad (\text{Compressibility}) \\ Q_0 &= 27\rho_0^3 \left. \frac{\partial^3 \mathcal{E}/\rho_B}{\partial \rho_B^3} \right|_{\rho_B=\rho_0, y_p=1/2} \quad (\text{Skewness coefficient}) \end{aligned} \quad (26)$$

and the volume part of the iso-spin incompressibility

$$K_{\tau,v} = K_{sym}^0 - 6L^0 - \frac{Q_0}{K_0} L^0. \quad (27)$$

We have assumed $K_{\tau,v} = K_\tau$ since the volume term is dominant [19]. These parameters characterize the density dependence of nuclear symmetry energy around normal nuclear matter density and thus provide important information on the behavior of nuclear symmetry energy at both high and low densities. Also, the curvature parameter K_{sym}^0 distinguishes the different parametrizations. A more significant measurement would be the evaluation of the shift of the incompressibility with asymmetry, which is given by

$$K_{asy} = K_{sym}^0 - 6L^0 \quad (28)$$

because this value can be correlated to experimental observations of the giant monopole resonance (GMR) of neutron-rich nuclei. Recent observations of the GMR [2] on even- A Sn isotopes give a quite stringent value of $K_{asy} = -550 \pm 100$ MeV. In the present model we determine this value for three quark masses of 300, 40, and 5 MeV and observe that they are consistent with the GMR measurements.

The compressibility K_0 at saturation density can be determined analytically, from Eq. (26):

$$K_0 = 9 \left(\frac{g_\omega}{m_\omega} \right)^2 \rho_0 + \frac{3k_{f,N}^2}{E_{f,N}^*} + \frac{3k_{f,N}M_N^*}{E_{f,N}^*} \cdot \frac{dM_N^*}{dk_{f,N}}. \quad (29)$$

The study of the correlation between symmetry energy and its slope can be performed analytically. For this purpose we use the Eqs. (16) and (23) to find \mathcal{E}_{sym} . In this model, we get the closed-form expression

$$L^0 = 3J + f(M_N^*, \rho_0, B_0, K_0), \quad (30)$$

where

$$f(M_N^*, \rho_0, B_0, K_0) = \frac{1}{2} \left(\frac{3\pi^2}{2} \right)^{2/3} \frac{1}{E_{f,N}^*} \times \left[\left(\frac{g_\omega}{m_\omega} \right)^2 \frac{\rho_0^{5/3}}{E_{f,N}^*} - \frac{\rho_0^{2/3} K_0}{9E_{f,N}^*} - \frac{\rho_0^{2/3}}{3} \right]. \quad (31)$$

The correlation function $f(M_N^*, \rho_0, B_0, K_0)$ exhibits the dependence on the different bulk parameters M_N^*, ρ_0, B_0 , and K_0 .

IV. STABILITY CONDITIONS

Nuclear forces have an attractive long-range part and a repulsive hard core similar to a Van der Waals fluid. It is expected to present a liquid and a gas phase characterized by the respective densities. Nucleons can be either protons or neutrons. Such a two-component system undergoes liquid-gas phase transition. The asymmetric nuclear matter (ANM) shows two types of instabilities [20]: a mechanical instability conserving the proton concentration and a chemical instability occurring at constant density.

We consider asymmetric nuclear matter characterized by proton and neutron densities $\rho_N = \rho_p, \rho_n$ and transform these into a set of two mutually commuting charges $\rho_i = \rho_B, \rho_3$ [21]. In infinite matter the extensivity of free-energy implies that it can be reduced to a free energy density: $\mathcal{F}(T, \rho_i) = \mathcal{E} - TS$ which at $T = 0$ reduces to energy density \mathcal{E} only. Since, we deal with a two-component nuclear medium, spinodal instabilities are intimately related to phase equilibria and phase transitions. Although it consists of unstable states, the spinodal region of the phase diagram can be addressed by standard thermodynamics.

The condition for stability implies that the free energy density is a convex function of the densities ρ_i . A local necessary condition is the positivity of the curvature matrix:

$$\mathcal{F}_{ij} = \left(\frac{\partial^2 \mathcal{F}}{\partial \rho_i \partial \rho_j} \right)_T \equiv \left(\frac{\partial \mu_i}{\partial \rho_j} \right)_T. \quad (32)$$

Here we used $\frac{\partial \mathcal{F}}{\partial \rho_i} \Big|_{T, \rho_{j \neq i}} = \mu_i$, where the effective chemical potentials in the present context are given by

$$\begin{aligned} \mu_p &= \sqrt{k_{f,p}^2 + M_p^{*2}} + V_\omega + \frac{1}{2} V_\rho, \\ \mu_n &= \sqrt{k_{f,n}^2 + M_n^{*2}} + V_\omega - \frac{1}{2} V_\rho. \end{aligned} \quad (33)$$

m_q (MeV)	g_σ^q	g_ω	g_ρ	$a(\text{fm}^{-3})$	$V_0(\text{MeV})$
5	6.44071	2.39398	9.04862	0.978629	111.265238
40	5.46761	3.96975	8.99036	0.892380	100.187229
300	4.07565	9.09078	8.51458	0.534296	-62.257187

TABLE I. Parameters for nuclear matter. They are determined from the binding energy per nucleon, $E_{B.E} = B_0 \equiv \mathcal{E}/\rho_B - M_N = -15.7$ MeV and pressure, $P = 0$ at saturation density $\rho_B = \rho_0 = 0.15 \text{ fm}^{-3}$.

Since we consider a two-fluid system, $[\mathcal{F}_{ij}]$ is a 2×2 symmetric matrix with two real eigenvalues λ_\pm [22]. The two eigenvalues are given by,

$$\lambda_\pm = \frac{1}{2} \left(\text{Tr}(\mathcal{F}) \pm \sqrt{[\text{Tr}(\mathcal{F})]^2 - 4\text{Det}(\mathcal{F})} \right), \quad (34)$$

and the eigenvectors $\delta \rho_\pm$ by

$$\frac{\delta \rho_i^\pm}{\delta \rho_j^\pm} = \frac{\lambda_\pm - \mathcal{F}_{jj}}{\mathcal{F}_{ji}}, \quad i, j = p, n. \quad (35)$$

The largest eigenvalue is always positive whereas the other can take on negative value. We are interested in the latter, because it defines the spinodal surface, which is determined by the values of T, ρ , and y_p . The smallest eigenvalue of \mathcal{F}_{ij} becomes negative. The associated eigenvector defines the instability direction of the system, in isospin space.

V. RESULTS AND DISCUSSION

We set the model parameters (a, V_0) by fitting the nucleon mass $M_N = 939$ MeV and charge radius of the proton $\langle r_N \rangle = 0.87$ fm in free space. Taking standard values for the meson masses; namely, $m_\sigma = 550$ MeV, $m_\omega = 783$ MeV and $m_\rho = 763$ MeV and fitting the quark-meson coupling constants self-consistently, we obtain the correct saturation properties of nuclear matter binding energy, $E_{B.E.} \equiv B_0 = \mathcal{E}/\rho_B - M_N = -15.7$ MeV, pressure, $P = 0$, and symmetry energy $J = 32.0$ MeV at $\rho_B = \rho_0 = 0.15 \text{ fm}^{-3}$. The values of g_σ^q, g_ω , and g_ρ obtained this way and the values of the model parameters at quark masses 5, 40, and 300 MeV are given in Table I. In Figs. 1(a) and 1(b), we plot the binding energy per nucleon for nuclear matter as a function of density corresponding to $m_q = 40$ MeV and $m_q = 300$ MeV, respectively, for different y_p values. In Fig. 2, we compare the variation of the binding energy per nucleon for quark mass 40 and 300 MeV with that of QMC and observe that, for 300 MeV, MQMC compares well with that of QMC. It is observed from Figs. 1 and 2 that, at low quark mass, the equation of state is softer. In Table II, we compare the nuclear matter properties at saturation for quark masses 5, 40, and 300 MeV, respectively,

TABLE II. Nuclear matter properties of the models used in the present work. The quantities presented are at saturation density.

Model	B_0 (MeV)	ρ_0 (fm $^{-3}$)	M^*/M	K_0 (MeV)	J (MeV)	L^0 (MeV)	K_{sym}^0 (MeV)	K_{asy} (MeV)	Q_0 (MeV)	K_τ (MeV)
MQMC (5 MeV)	-15.7	0.151	0.93	159	32.0	84.7	-27.7	-535.9	103.2	-590.8
MQMC (40 MeV)	-15.7	0.151	0.91	208	32.0	84.9	-28.4	-537.6	94.2	-575.9
MQMC (300 MeV)	-15.7	0.151	0.76	349	32.0	89.1	-14.5	-549.0	-15.6	-545.1
DD [23]	-16.0	0.149	0.56	239	31.6	55.9	-95.3	-431.1	576.8	-462.57
QMC [24, 28]	-15.7	0.150	0.77	291	33.7	93.5	-10.0	-570.8	29.4	-580.24
FSUGold [25]	-16.2	0.148	0.61	229	32.6	60.4	-51.4	-414.0	425.7	-276.07
BKA24 [26]	-15.9	0.147	0.60	227	34.2	84.8	-14.9	-523.7	112.4	-421.55
BSR12 [27]	-16.1	0.147	0.61	232	34.0	77.9	-44.2	-511.6	324.2	-414.30

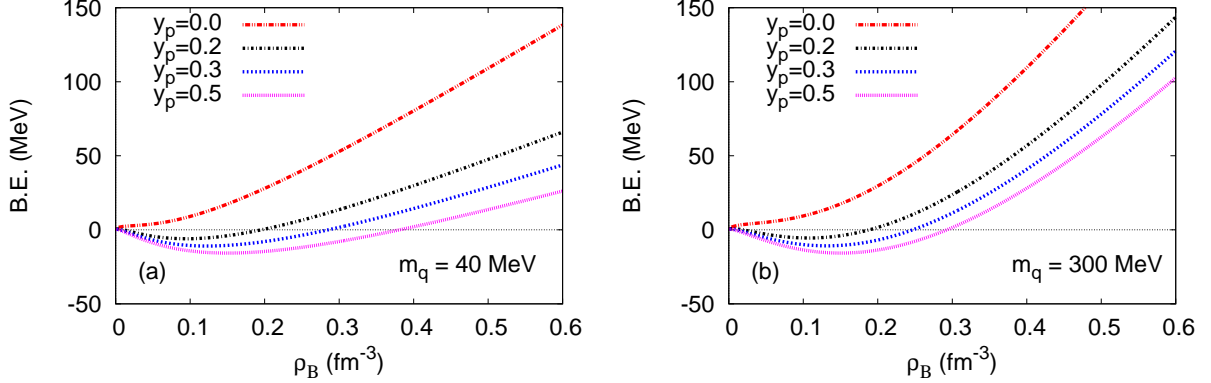


FIG. 1. (Color online) Nuclear matter binding energy as a function of density for (a) different y_p values for quark mass $m_q = 40$ MeV and (b) quark mass $m_q = 300$ MeV.

in the present model to QMC [24, 28], and some of the approved models as suggested in Ref. [19].

The value of the compressibility K_0 is determined to be 159, 208, and 349 MeV respectively, for quark masses 5, 40, and 300 MeV. A recent calculation [29] has predicted K_0 to be in the range $250 < K_0 < 315$ from the experimental GMR energies in even-even $^{112-124}\text{Sn}$ and $^{106,100-116}\text{Cd}$. Furthermore, the value of the effective mass calculated in the present model at quark mass 300 MeV is 0.76 which compares well with the empirical value of the effective mass, which is 0.74 [30].

We compare the symmetry energy, its slope, and incompressibility from our model with the QMC [24, 28] results respectively in Figs. 3(a), 3(b), and 3(c). We observe that the symmetry energy shows an extremely linear behavior. This is further justified from the plot for the slope parameter L . This is based on equation (23) for \mathcal{E}_{sym} . However, if we consider terms higher than the quadratic one in defining the relation in Eq. (22), it would be more appropriate to use the expression as in Eq. (24) to show the density dependence of \mathcal{E}_{sym} for higher nuclear densities ($\rho_B > \rho_0$). This has been shown in Fig. 4 in comparison with several other models, as noted there, including QMC.

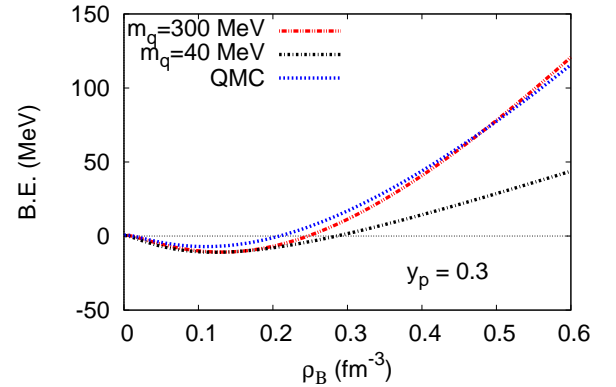


FIG. 2. (Color online) Nuclear matter binding energy as a function of density for quark mass $m_q = 40$ MeV and quark mass $m_q = 300$ MeV for $y_p = 0.3$. A comparison is made between the MQMC for quark mass 40 MeV and 300 MeV with that of QMC.

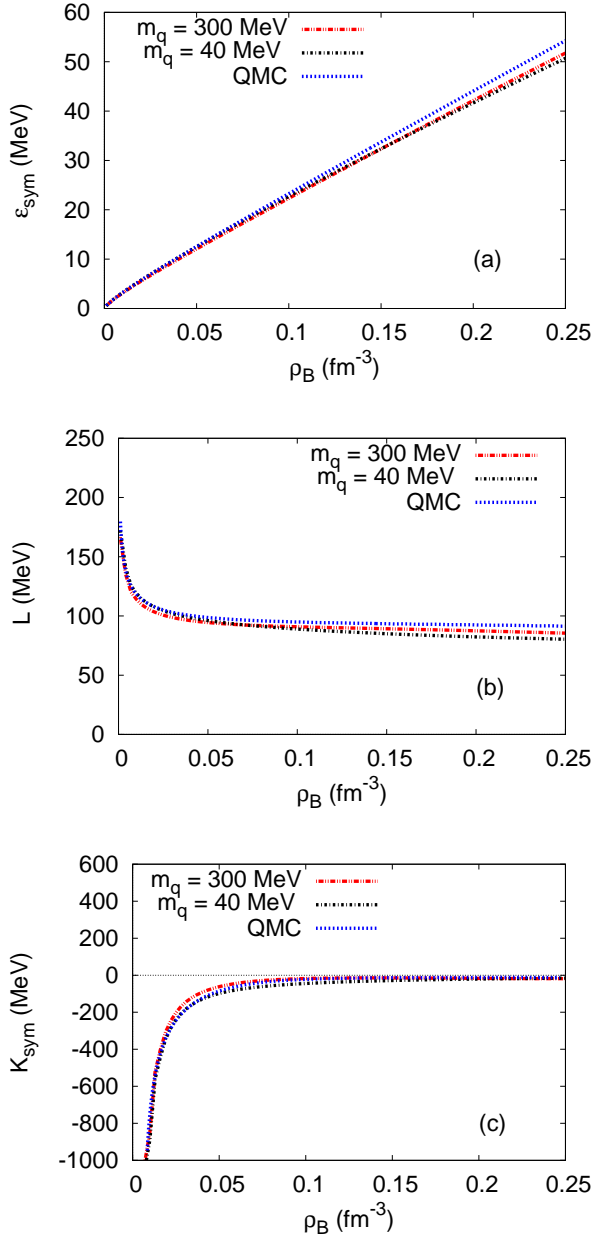


FIG. 3. (Color online) (a) Symmetry energy, (b) its slope parameter L , and (c) K_{sym} (c) in the MQMC and QMC models as functions of baryon density ρ_B

A. Correlation between the symmetry energy and its slope

We study the correlation function $f(M_N^*, \rho_0, B_0, K_0)$ with the variation of quark masses in Fig. 5. We observe that the function $f(M_N^*, \rho_0, B_0, K_0)$ increases with quark masses. The established value of binding energy B_0 and the saturation density ρ_0 in the nuclear mean-

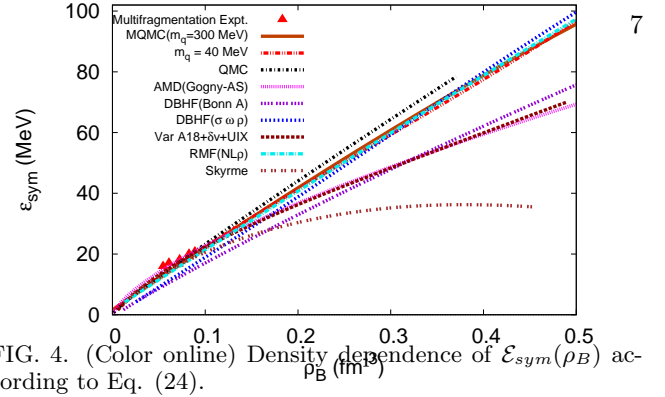


FIG. 4. (Color online) Density dependence of $\epsilon_{\text{sym}}(\rho_B)$ according to Eq. (24).

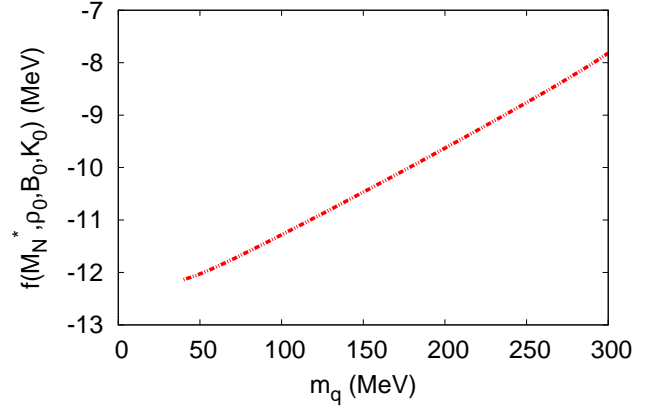


FIG. 5. (Color online) Correlation function $f(M_N^*, \rho_0, B_0, K_0)$ at various quark masses.

field models cannot be applied to incompressibility K_0 and effective mass M_N^* since the latter are found as output in this model where the coupling constants are fixed in a self consistent manner by taking into consideration the binding energy and saturation density. Therefore, we have taken the variation of f with different quark masses

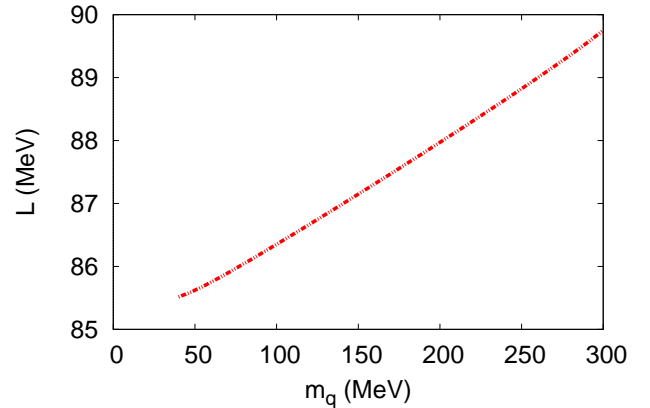


FIG. 6. (Color online) The slope of symmetry energy, L at various quark mass.

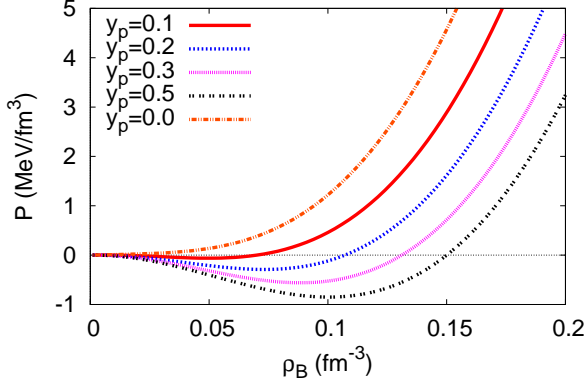


FIG. 7. (Color online) Pressure as a function of density at various isospin asymmetries.

at the same B_0 and ρ_0 . We observe that, because there is only one isovector parameter g_ρ^2 in the expression for \mathcal{E}_{sym} and L , the variation is linear. Such linearity in the behavior was also observed in nonrelativistic models [17]. It indicates one of the limitations of the model parameters. We expect a nonlinear behavior between \mathcal{E}_{sym} and L for the models with more than one isovector parameter. In the Fig. 6, we have shown the slope of symmetry energy, L at various quark masses. It is interesting to note that there is a linear relationship of the slope of the symmetry energy L with quark mass. This is a direct consequence of the dependence of the symmetry energy on g_ρ^2 .

B. Instability

We next study the mechanical instability and its dependence on the isospin asymmetry of the system by plotting the pressure as a function of density and the asymmetry parameter y_p . In Fig. 7, we show that the mechanical instability occurs in the region where the slope of the pressure with respect to density is negative. We observe that the mechanical-instability region shrinks when the isospin-asymmetry increases. The system is stable under separation of two phases if the free energy of a single phase is lower than the free energy in all two-phase configurations.

In the spinodal area we can get the signature of the mechanical instability by finding the velocity of sound determined in the model as

$$\beta^2 = \frac{dP}{d\mathcal{E}} = \frac{dP}{d\rho_B} / \frac{d\mathcal{E}}{d\rho_B}, \quad (36)$$

where $\beta^2 = v_s^2/c^2$, v_s is the velocity of sound and c is the speed of light. In Fig. 8 we show the sound velocity as a function of density by changing the asymmetry parameter. There is a reduction in the instability when we

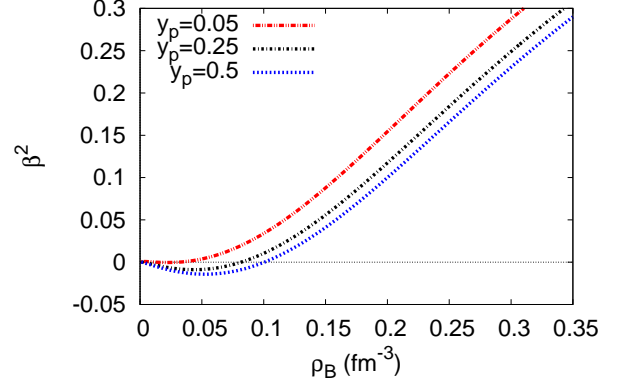


FIG. 8. (Color online) Sound velocity as a function of density.

move away from the symmetric nuclear matter. Moreover, the velocity becomes imaginary when we enter into the spinodal area [21].

The positivity of the local curvature matrix is equivalent to the condition that both the trace $Tr[\mathcal{F}_{ij}] = \lambda_+ + \lambda_-$ and the determinant $det[\mathcal{F}_{ij}] = \lambda_+ \lambda_-$ are positive. In the present model the above condition is violated and the system is in the unstable region of a phase transition. Further it is to be pointed out that for a two component, n-p thermodynamical system, the stability parameter is given by the condition;

$$S_P = \left(\frac{\partial P}{\partial \rho_B} \right)_{T, y_p} \cdot \left(\frac{\partial \mu_p}{\partial y_p} \right)_{T, P} > 0, \quad (37)$$

but in charge symmetric matter the isoscalar (total density) $\delta\rho_n + \delta\rho_p$ and isovector (concentration) $\delta\rho_n - \delta\rho_p$ oscillations are not coupled and there are two separate conditions for instability [31]. These conditions are for mechanical instability

$$\left(\frac{\partial P}{\partial \rho_B} \right)_{T, y_p} \leq 0, \quad (38)$$

and for chemical instability

$$\left(\frac{\partial \mu_p}{\partial y_p} \right)_{T, P} \leq 0. \quad (39)$$

In the ANM the isoscalar and isovector modes are coupled and the two separate inequalities do not select the nature of instability. Moreover, we observe in Fig. 9, a large difference in the behavior of the stability parameter S_P in Eq. (37) inside the instability region. For higher asymmetry, the range of the stability parameter is smaller than at lower asymmetries. To understand this effect we follow the Landau-dispersion-relation approach for small-amplitude oscillations in Fermi liquids [32]. For a two component (n, p) matter, the interaction is characterized by the Landau parameters $F_0^{q,q'}$ which is defined

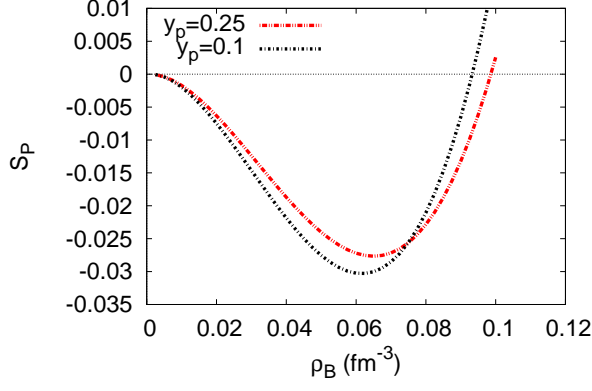


FIG. 9. (Color online) The stability parameter S_p [Eq. (37)] as a function of ρ_B for $y_p = 0.25$ and $y_p = 0.1$ in the instability sector.

by the relationship

$$N_q(T) \frac{\partial \mu_q}{\partial \rho_{q'}} \equiv \delta_{q,q'} + F_0^{q,q'}, \quad (40)$$

where $q = (n, p)$ and $N_q(T)$ represents the single-particle level density at the Fermi energy. At zero temperature it has the simple form

$$N_q = \frac{k_{Fq} E_{Fq}^*}{\pi^2}. \quad (41)$$

In the symmetric case ($F_0^{nn} = F_0^{pp}$, $F_0^{np} = F_0^{pn}$), the Eqs. (38) and (39) correspond to the two Pomeranchuk instability conditions

$$\begin{aligned} F_0^s &= F_0^{nn} + F_0^{np} < -1 & \text{mechanical} \\ F_0^a &= F_0^{nn} - F_0^{np} > -1 & \text{chemical} \end{aligned} \quad (42)$$

The dispersion relations F_0^s give the properties of density (isoscalar) modes and F_0^a gives the concentration (isovector) modes.

In the unstable region of dilute asymmetric nuclear matter we have isoscalar-like unstable modes, hence $1 + F_0^s < 0$, while the combination $1 + F_0^a > 0$. In the Fig. 10 we plot the values obtained from the calculation of these two quantities in the unstable region at zero temperature for $y_p = 0.25$. An important observation we make from the comparison of Figs. 9 and 10 is the shift in the maximum instability density region. In Fig. 9 the largest instability (the most negative value) is at $\rho_B = 0.065 \text{ fm}^{-3}$. However, the most negative Pomeranchuk condition $1 + F_0^s$, which corresponds to the fastest unstable mode, is present in more dilute matter at $\rho_B = 0.03 \text{ fm}^{-3}$.

In the following we study the direction of instability of the system. In Fig. 11, we show the ratio of the proton versus neutron density fluctuations corresponding to the unstable mode which defines the direction of instability

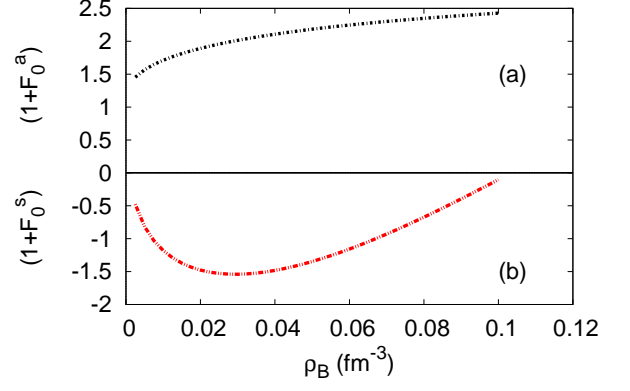


FIG. 10. (Color online) Behavior of generalized Landau parameters (a) $1 + F_0^a$ (b) $1 + F_0^s$ with respect to baryon density ρ_B in the instability sector for $y_p = 0.25$.

of the system. We plot the results for different proton fractions and observe that the instabilities tend to restore the isospin symmetry for the dense (liquid) phase leading to the fractionation of the ANM.

Figure 12 shows the proton-neutron density fluctuation ratio as a function of the isospin asymmetry for a fixed nuclear density, $\rho = 0.06 \text{ fm}^{-3}$ and compares it to the QMC and Brueckner-Hartree-Fock (BHF) calculations. The relativistic models give larger fluctuation ratios than the corresponding value of ρ_p/ρ_n . We also observe that the fluctuation ratio in the present model is larger compared to the nonrelativistic BHF model. A pure mechanical disturbance would occur [20] if the instability preserves the ratio between protons and neutrons, i.e., $\frac{\delta \rho_p^-}{\delta \rho_n^-} = \frac{\rho_p}{\rho_n}$. Conversely if $\delta \rho_p^- = -\delta \rho_n^-$ then we should observe pure chemical disturbance. In the present case we observe that the disturbance along the unstable eigen direction conserves neither ρ nor y_p but has mixed character with both chemical and mechanical contents.

C. Constrain on neutron star radii

The symmetry energy plays an important role in describing the mass-radius relationship in neutron stars. Neutron stars are compact objects maintained by the equilibrium of gravity and the degeneracy pressure of the fermions together with a strong nuclear repulsion force due to the high density reached in their interior. The slope of the symmetry energy, L , constrains the neutron star radii. It is confirmed that the radii for the neutron stars with canonical mass $1.4 M_\odot$ are not affected by the symmetry energy at saturation density [33]. However, in some cases the radii increase with L , while in others, there is a decrease. In fact the radii are correlated with a variation of the slope L . The radii increase up to a

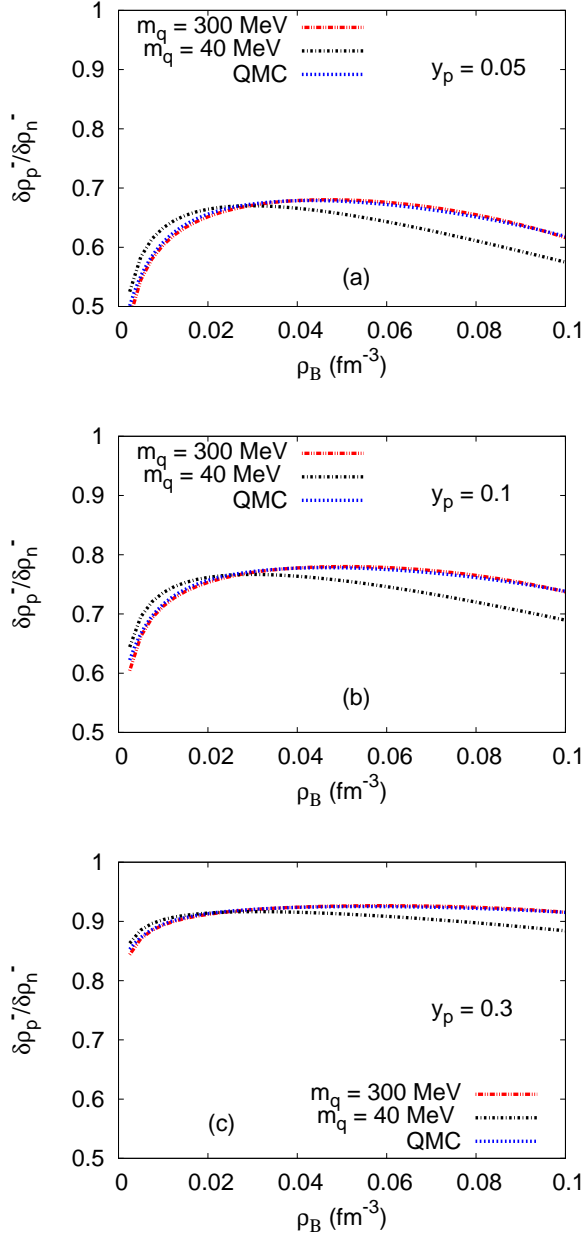


FIG. 11. (Color online) Ratio of proton-neutron density fluctuation corresponding to the unstable mode showing the direction of instability for (a) $y_p = 0.05$, (b) $y_p = 0.1$, and (c) $y_p = 0.3$.

maximum value, then drop again. This behavior can be associated with a maximum theoretical value of L , and provide a possible constraint to nuclear matter. In the present model the value of L^0 comes out to be 89 MeV which is very close to the experimental observation [2]. The most direct connection between the astrophysical observations and the nuclear symmetry energy concerns neutron star radii (R) which are highly correlated with

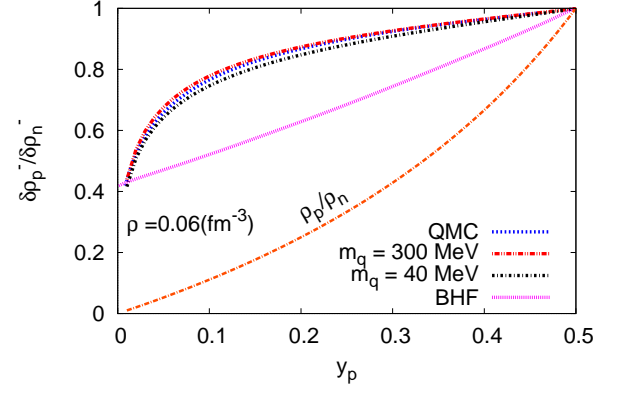


FIG. 12. (Color online) Proton-neutron density fluctuation ratio versus proton fraction y_p for a fixed nuclear density.

neutron star pressures near ρ_0 . It is to be noted that Latimer and Prakash [34] found the radii of neutron stars for masses near the canonical mass $1.4M_\odot$, obey a power-law relation:

$$R(M) = C(\rho, M)(P(\rho)/\text{MeV fm}^{-3})^{1/4} \quad (43)$$

where $R(M)$ is the radius of a star, $P(\rho)$ is the pressure of neutron star matter at density ρ , and $C(\rho, M)$ is a constant for a given density and mass. Considering the structure of a neutron star as pure neutron matter, the value of this constant at quark mass 300 MeV in our model comes out to be

$$C(2\rho_0, 1.4M_\odot) = 5.90\text{km} \quad (44)$$

which is very near to 5.68 ± 0.14 km predicted by Latimer *et al.* [34]. It is to be noted that the mass of the neutron star for pn matter with β equilibrium comes out to be $2.7 M_\odot$ with quark mass 300 MeV and $1.64 M_\odot$ with quark mass 40 MeV. The details of such calculations incorporating the hyperons in the composition of neutron stars is in progress.

VI. CONCLUSION

In the present work we have studied the EOS for asymmetric nuclear matter by using a modified quark-meson coupling model (MQMC). Self-consistent calculations were made by using a relativistic quark model with chiral symmetry along with the spurious center-of-mass correction, pionic correction for restoration of chiral symmetry, and short-distance correction for one-gluon exchange to realize different bulk nuclear properties. The instability in the two-component nuclear system is then analyzed. In asymmetric matter the isoscalar and isovector modes are coupled and the two separate inequalities for density oscillations and concentration oscillations no

longer maintain a physical meaning for the selection of the nature of the instabilities.

The symmetry energy, its slope (L), and curvature parameter (K_{sym}) were found in reasonable agreement with experimental values. Without considering self interactions in the scalar field, we found an analytic expression for the symmetry energy \mathcal{E}_{sym} as a function of its slope L . Our result establishes a linear correlation between L and \mathcal{E}_{sym} . We also study the variation of correlation function $f(M_N^*, \rho_0, B_0, K_0)$ with the variation of quark masses. The symmetry energy is correlated with neutron

star radii. In this model we observe that, at twice the saturation density ($0.3 fm^{-3}$), the constant $C(2\rho_0, M)$ is found 5.90 km in the canonical-mass region of $1.4M_\odot$.

ACKNOWLEDGMENTS

The authors would like to acknowledge the financial assistance from BRNS, India for the Project No. 2013/37P/66/BRNS.

-
- [1] M. Prakash, I. Bombaci, M. Prakash, P. J. Ellis and J. M. Lattimer, Phys. Rep. **280**, 1 (1997).
 - [2] T. Li, et al., Phys. Rev. Lett. **99** 162503 (2007); Bao-An Li, Lie-Wen Chen, Che Ming Ko, Phys. Repts. **464**, 113 (2008).
 - [3] G.A. Lalazissis, J. König, P. Ring, Phys. Rev. C **55**, 540 (1997).
 - [4] P. A. M. Guichon, Phys. Lett. B **200**, 235 (1988); P.A.M. Guichon, K. Saito, E. Rodionov, A.T. Thomas, Nucl. Phys. A **601** (1996) 349.
 - [5] K. Saito and A.W. Thomas, Phys. Lett. B **327**, 9 (1994); **335**, 17 (1994); **363**, 157 (1995); Phys. Rev. C **52**, 2789 (1995); K. Saito, K. Tsushima, and A.W. Thomas, Nucl. Phys. A **609**, 339 (1996); Phys. Rev. C **55**, 2637 (1997); Phys. Lett. B **406**, 287 (1997).
 - [6] P. G. Blunden and G.A. Miller, Phys. Rev. C **54**, 359 (1996); N. Barnea and T.S. Walhout, Nucl. Phys. A **677**, 367 (2000); H. Shen and H. Toki, Phys. Rev. C **61**, 045205 (2000); P.K. Panda, R. Sahu, C. Das, Phys. Rev. C **60**, 38801 (1999); P.K. Panda, M.E. Bracco, M. Chiapparini, E. Conte, and G. Krein, Phys. Rev. C **65**, 065206 (2002); P.K. Panda, and F.L. Braghin, Phys. Rev. C **66**, 055207 (2002).
 - [7] P.K. Panda, A. Mishra, J.M. Eisenberg, and W. Greiner, Phys. Rev. C **56**, 3134 (1997); I. Zakout, and H.R. Jaqaman, Phys. Rev. C **59**, 962 (1999).
 - [8] G. Krein, D.P. Menezes, M. Nielsen, and C. Providência, Nucl. Phys. A **674**, 125 (2000), P.K. Panda, G. Krein, D.P. Menezes and C. Providência, Phys. Rev. C **68**, 015201 (2003); P.K. Panda, D.P. Menezes, C. Providência, Phys. Rev. C **69**, 025207 (2004).
 - [9] T. Frederico, B. V. Carlson, R. A. Rego, M. S. Hussein, J. Phys. G **15**, 297 (1989).
 - [10] N. Barik and B.K. Dash, Phys. Rev. D **33**, 1925 (1986), *ibid*, Phys. Rev. D **34**, 2092 (1986); N. Barik and R.N. Mishra, Phys. Rev. D **61**, 014002 (2000),
 - [11] E.F. Batista, B.V. Carlson and T. Frederico, Nucl. Phys. A **697**, 469 (2002).
 - [12] N.Barik, B.K.Dash and M.Das, Phys. Rev. D **31**, 1652 (1985) *ibid* **32**, 1725 (1985); **34**, 2803 (1986). N.Barik, P.C.Dash, A.R.Panda, Phys. Rev. D **46**, 3856 (1992); N.barik, P.C. Dash, Phys. Rev. D **49**, 299 (1994).
 - [13] N. Barik, R. N. Mishra, D. K. Mohanty, P. K. Panda and T. Frederico, Phys. Rev. C **88** 015206 (2013).
 - [14] C. Ducoin, J. Margueron, C. Providência and I. Vidãna, Phys. Rev. C **83**, 045810 (2011).
 - [15] J. R. Stone and P.G. Reinhard, Prog. Part. Nucl. Phys. **58**, 587 (2007).
 - [16] L. W. Chen, C.M. Ko, Bao-An Li, and J. Xu, Phys. Rev. C **82**, 024321 (2010).
 - [17] B. M. Santos and M. Dutra, O. Lourenco and A. Delfino Phys. Rev. C **90** 035203 (2014).
 - [18] A. W. Steiner, Phys. Rev. C **74** 045808 (2006)
 - [19] M. Dutra *et al*, Phys. Rev. C **90**, 055203 (2014)
 - [20] P. Chomaz, M. Colonna and J. Randrup, Phys. Rep. **389** 263 (2004).
 - [21] J. Margueron and P.Chomaz, Phys. Rev. C **67** 041602 (2003).
 - [22] H. Müller and B. D. Serot, Phys. Rev. C **52** 2072 (1995).
 - [23] S. Typel, Phys. Rev. C **71**, 064301 (2005)
 - [24] A.M. Santos C. Providência, P.K. Panda, Phys. Rev. C **79**, 045805 (2009).
 - [25] B.G.Todd-Rutel and J. Piekarewicz, Phys. Rev. Lett. **95**, 122501 (2005)
 - [26] B.K.Agrawal, Phys. Rev. C **81**, 034323 (2010)
 - [27] S. K. Dhiman, R. Kumar and B. K. Agrawal, Phys. Rev. C **76**, 045801 (2007)
 - [28] P.K. Panda, A.M. Santos, D.P. Menezes, C. Providência, Phys. Rev. C **85**, 055802 (2012).
 - [29] J.R.Stone, N. J. Stone and S. A. Moszkowski, Phys. Rev. C **89**, 044316 (2014)
 - [30] M. Jaminon and C. Mahaux, Phys. Rev. C **40**, 354 (1989)
 - [31] B. Liu, V. Greco, V. Baran, M. Colonna, and M. Di Toro, Phys. Rev. C **65**, 045201 (2002).
 - [32] L.D. Landau and E.M. Lifshitz, *Statistical Physics* (Pergamon Press Ltd., Oxford, England, 1981) page 208; G. Baym and C. Pethick, *Landau Fermi-liquid theory* (John Wiley and Sons, New York, 1991); L.Scalone, M.Colonna and M.Di Toro, Phys. Lett. B **461**, 9 (1999).
 - [33] L.L.Lopes and D.P.Menezes, Braz. J. Phys. **44**, 774 (2014).
 - [34] J. M. Lattimer and Y. Lim, Astrophys. J. **771** 51 (2013).